LORCA: A High Performance USV with Applications to Surveillance and Monitoring

Joachim Grenestedt[1] Jack Keller[2*] Scott Larson[1] Jake Patterson[1] John Spletzer[2] Tyler Trephan[2]
[1]Department of Mechanical Engineering
[2]Department of Computer Science and Engineering
Lehigh University
[*]Lehigh University, 19 Memorial Drive West, Bethlehem, PA 18015, e-mail: jfk214@lehigh.edu

***Abstract*—In this paper, we introduce the Lehigh Ocean Research Craft Autonomous (LORCA) - a high performance USV with applications to surveillance and monitoring tasks. Compact (1.2 m), lightweight (5 kg) and robust (one-piece carbon fiber design), LORCA is capable of speeds of 80 kph (50 mph). It was also designed to be capable of operations in ocean waves, with self-righting ability in all sea states. We first review the LORCA design and technical specifications. We then discuss our initial work in trajectory following where an EKF-based approach is employed for localization and a sample based planner for control. Using only the sensing and computational resources available on a 3DR Pixhawk, we demonstrate effective trajectory following in a riverine environment at peak speeds of 48 kph (30 mph). We conclude with discussions on the limitations of the current approach and planned future work.**

Fig. 1: LORCA USV developed at Lehigh University. The vehicle features a top speed of 80 kph. In autonomous operations, top speeds of 48 kph were demonstrated during a trajectory following task.

I. Introduction

Maritime robotics is a quickly evolving field, with significant interest not only in academia [1]–[9] but also by commercial concerns [10], [11]. Most of popular media success stories in this arena relate to the exploits of autonomous underwater vehicles (AUVs), and gliders in particular. This is understandable, as glider AUVs have demonstrated long-term autonomy for hundreds of days while traveling thousands of kilometers. As an example, in 2009 Scarlet Knight, a 2.4 meter (8 foot) autonomous glider, made headlines by becoming the first robot to successfully cross the Atlantic Ocean [12]. In 2013, the Rutgers Center for Ocean Observing Leadership reported that the Challenger mission had 2 gliders which traveled over 15,000 km in over 803 days as of 2013 [13], [14]. There are numerous other groups working with gliders, and the U.S. Integrated Ocean Observing System (IOOS) reported that its regional and industry partners have flown over 15,000 glider days in the past 3 years alone [15]. Gliders are able to achieve such feats as they can make many of the same simplifying assumptions that UAVs do when flying. Specifically, they operate in a three-dimensional space that is assumed to be free of obstacles. This mitigates the need for exteroceptive sensors and the associated algorithms to handle collision detection and avoidance. Indeed, Scarlet Knight's crossing had to be closely coordinated with fishermen to ensure the vehicle would not become fishing net by-catch [12].

In contrast, advances in unmanned surface vehicles (USVs) - *aka* autonomous surface vehicles (ASVs) - have been slower. Unlike AUVs, the operational environment of USVs is approximately two-dimensional. As a result, the potential for collisions with obstacles or other vehicles is far higher. Ultimately, collision detection and avoidance modalities for USVs will be a necessity in many applications. Furthermore, operations in the presence of waves (e.g., in the ocean) motivates the need for real-time reconstruction of the water surface. An analogy to unmanned ground vehicles (UGV) would be operations in cross-country terrain, where terrain classification would allow the vehicle to navigate more safely and effectively. Unfortunately, the primary sensors used in terrestrial robots are unsuitable for this task. Light from LIDAR systems is largely absorbed and lack of consistent structure/texture renders stereo vision ineffective. The impact of waves on vehicle navigation can be mitigated in part through vehicle design, and we have taken such an approach.

To this end, we introduce the Lehigh Ocean Research Craft Autonomous (LORCA) - a high performance USV with applications to surveillance and monitoring. Compact (1.2 m), lightweight (5 kg) and robust (one-piece carbon fiber design), LORCA is capable of speeds of 80 kph (50 mph). It was also designed to be capable of operations in ocean waves, with self-righting ability in all sea states. In the remainder of this paper, we first review the LORCA design and technical specifications in Section III. In Section IV, we discuss our initial work in trajectory following where an EKF-based approach is employed for localization and a sample based planner for control. In Section V, we provide experimental results which demonstrate effective trajectory following in a riverine environment at peak speeds of 48 kph (30 mph). Finally, in Section VI we conclude with discussions on the limitations of the current approach and planned future work.

II. Related Work

Recently, there has been increased research attention to USVs. Environmental monitoring is an application area of significant interest. Research on collecting marine biology data and bathymetry has focused on both operations in the sea and operations in shallower regions closer to shore in smaller bodies of water. In [1] and [3], both focus on vehicles designed to gather data at sea and function for a long duration by taking advantage of wind, solar power, and using waves to harness energy. Carnegie Mellon University has developed a low cost fleet of small airboats which are capable of autonomously monitoring water quality in lakes [6]. Teams of larger boats capable of swapping out their sensor payloads have also been developed and tested by measuring greenhouse gases emitted from a lake [8]. These USVs were 1.5 meters in length with a top speed of 8 kph. There has also been research done into using a team of robots to track an invasive species of carp tagged with radio transmitters [5].

USVs also have safety, security, and rescue applications. In [9], a 1 meter catamaran was used to gather images in lakeshore environments and monitor changes in the environment. It operated with a top speed of 7 kph. A catamaran style USV called ROAZ was developed to assess risks in shoreline environments [2]. There has also been research into using a 4.7 meter long rigid-hulled inflatable boat (RHIB) to detect and remove mines [4]. Arrichiello *et al* have developed a strategy for a pair of USVs attached together with a rope to capture and transport a target to a destination, which has applications in rescue operations [7].

As navigating reliably through its environment is necessary for most applications of USVs, there has also been significant research on path and trajectory following. The problem is challenging since USVs operating in water are underactuated. In [16], a Kalman Filter was used for position estimation along with a PD controller on the USV's heading and a PI controller for velocity. In [17], the USV's actual position was projected on the path to be followed and the path is followed by minimizing the difference between the USV's actual and desired position and orientation. [18] develops trajectory and path following controllers for USVs even when there is uncertainty in the parameters of the USV's model. The USVs used to test in these papers were a hovercraft [18], catamaran [16], and simulation [17].

From this review, we found that USVs used in academic research in shallow, shoreline environments are typically small, often catamarans, and operate at relatively modest speeds. In contrast, LORCA was designed to have a compact size while providing high performance and a robust design capable of operations in both shallow water and in the ocean under a range of seat states.

III. Development Platform

One of the goals of the LORCA project was to develop a high-performance USV platform suitable for a range of surveillance and monitoring tasks. However, an underlying requirement which largely shaped vehicle design was the ability to operate in the ocean under at least sea state 4 conditions. To this end, several different hull designs were evaluated. This included testing of available high-end commercial-off-the-shelf (COTS) model boats. However, these proved of inferior quality for the form factor and intended purpose. Neither the hull/deck nor the hardware were built to industrial standards. As a result, a major effort was made to design and build our own boats and essentially all hardware. The resulting vehicle platform is shown in Figure 2.

Fig. 2: LORCA boat Number 1. The single piece carbon fiber design is both strong and lightweight. The stepped mono-hull reduces drag.

A strong yet lightweight hull for all-weather operation was desired, so the boats were manufactured as one-piece and of carbon fiber using autoclave cured prepreg. The stepped mono-hull was chosen for reduced drag, and can accommodate a large range of center of mass locations longitudinally. The finished vehicle has a length of 1.2 meters, and a base weight of 5 kg (single battery set, no on-board computing, no sensor payload). The tall rounded deck design also provides self-righting abilities in all sea states. A demonstration of self-righting is illustrated at Figure 3.

The hardware for outfitting the USV's was mostly designed inhouse and CNC machined from high-quality materials. Brushless in-runner electric motors were the powerplant of choice. In particular LORCA Number 1 (featured herein) has a Neu 2230 motor rated to 5 kW continuous/10 kW burst. With this motor/driveline combination, top speed has been measured at 80 kph (50 mph). Access to the interior is through a single plexiglass window. A total of four batteries can can be accommodated, which provides approximately 40 minutes of run time at a cruising speed of 30 kph. There is also substantial room for additional payload, and we estimate a 5kg payload can be accommodated with no significant loss in maneuverability.

Finally, we note that in its current state of development, the only on-board computing is the 3DR PixHawk autopilot system [19]. This will change in the near future, but as of this

Fig. 3: Aerial launch of a fully loaded and functional LORCA USV demonstrating its self-righting capabilities.

writing all of the planning, estimation and control algorithms outlined in this manuscript reside locally on the PixHawk.

IV. Trajectory Following

Our initial efforts in vehicle autonomy were the development of trajectory following behaviors, i.e., following a desired path in time. For purposes of this work, a trajectory $T = \{(x_1, y_1, t_1), \dots, (x_k, y_k, t_k)\}$ was parameterized by a sequence of k 2D waypoints (x, y) each with an associated time-of-arrival (TOA) t. The objective of trajectory following is then to reach each of these waypoints as near to the specified TOA as possible. The remainder of this section outlines our approaches to perception, planning, and control to achieve effective trajectory following at speeds of 20-50 kph.

A. Localization

Currently, LORCA relies entirely upon the 3DR Pixhawk autopilot system for both sensing and computation. This implies a heavy reliance on GPS for localization. However, the limited update rate (5 Hz) was deemed insufficient for the intended operational speeds of the craft. As a result, we implemented an Extended Kalman Filter (EKF) which integrated linear and angular velocity estimates from both the GPS and the on-board gyroscopes to increase the feedback control loop to 10 Hz.

The state transition model for the time update phase is defined in terms of the previous state and the linear and angular velocities of the USV as in [16]

$$\begin{bmatrix} x \\ y \\ \theta \end{bmatrix}_{k+1} = \begin{bmatrix} x \\ y \\ \theta \end{bmatrix}_{k} + \begin{bmatrix} v_k \cos(\theta_k + d\theta) + \dot{x_c} \\ v_k \sin(\theta_k + d\theta) + \dot{y_c} \\ \omega_k \end{bmatrix} \Delta t \tag{1}$$

where $[x, y, \theta]^T$ is the position and orientation (yaw) of the USV in an earth-fixed frame, v is the linear (surge) velocity of the vessel with respect to the water, ω is the yaw rate, $[\dot{x}_c, \dot{y}_c]^T$ is the current, and Δt is the period of the USV's feedback control loop. Note this model assumes vehicle motion is planar, and the effects of pitch and roll can be ignored. Such a simplification was justified in [20]. It further assumes that the sway (lateral) velocity of the USV can be neglected, which is also a common assumption in the literature. Since we currently do not have a sensor to measure surge speed in the water, we further assume that $\dot{x_c} = \dot{y_c} = 0$ so that v is estimated directly from GPS. We note again that this simplified model has limitations when applied to a highly dynamic USV such as LORCA. This is discussed in greater detail in Section V.

The Jacobian of the state transition function with respect to the state is defined as

$$A = \begin{bmatrix} 1 & 0 & -v_k \sin(\theta_k + d\theta)\Delta t \\ 0 & 1 & v_k \cos(\theta_k + d\theta)\Delta t \\ 0 & 0 & 1 \end{bmatrix}$$

and the Jacobian of the state transition function with respect to the process noise is defined as

$$W = \begin{bmatrix} \cos(\theta_k + d\theta)\Delta t & -v_k \sin(\theta_k + d\theta)\Delta t/2 \\ \sin(\theta_k + d\theta)\Delta t & v_k \cos(\theta_k + d\theta)\Delta t/2 \\ 0 & \Delta t \end{bmatrix}$$

For the measurement update phase, the observation $z_k = [x_k, y_k, \theta_k]^T$ is the 2D position and orientation of the USV as estimated directly by the GPS. As a result, the associated Jacobians H and V are identity matrices.

The process then follows a traditional EKF implementation with the time update phase running at 10 Hz, while the measurement update rate is GPS limited at 5 Hz.

B. Velocity Control

To regulate the linear and angular velocities of LORCA, we created a mapping to the vehicle's steering and throttle positions. This was done during a calibration phase where open-loop actuator commands were sent to the throttle and steering, and the steady-state velocities were measured using the autopilot sensors. The resulting mappings were implemented as a pair of lookup tables (LUT) which were populated by performing bilinear interpolation over the calibration data. A sample LUT for throttle position is shown at Figure 4. This is indexed by the specified linear and angular velocities (v_d, ω_d) to obtain the required throttle setting. A similar LUT exists for rudder position.

To improve tracking performance, we are currently using a proportional controller on linear velocity. The angular velocity signal is based upon the open-loop response. The justification for this was that if the actual linear velocity was correct, the angular velocity would be consistent as it is driven by the rudder position. This was done for expediency, and we are currently refining this approach.

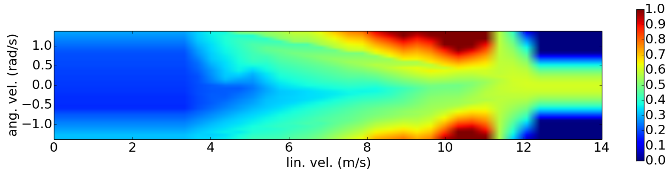

Fig. 4: LUT used to select throttle position. In this instance, the feasible set of angular velocities was artificially constrained for high linear velocities.

C. Planning

The role of the planner was to specify the desired linear and angular velocities (v_d, ω_d) for trajectory following. These in turn serve as input to the controller described in Section IV-B. The solutions we have reviewed in Section II typically relied upon analytical solutions/control laws to solve the path planning problem. Instead, we take inspiration from successes in terrestrial robotics [21], and propose a sample-based approach to path following.

Planning was done on the input space of linear and angular velocities in two stages. Given the robot position (x_r, y_r) at time t and the current target waypoint (x_g, y_g, t_g), the desired velocity v_d was specified simply as

$$v_d = \begin{cases} \min\left(\frac{\|(x_r - x_g, y_r - y_g)\|}{t_g - t}, v_{max}\right), & \text{if } t_g \geq t \\ v_{max}, & \text{otherwise} \end{cases} \quad (2)$$

where v_{max} is the maximum allowable surge velocity for the LORCA. In other words, the velocity is chosen that will allow the boat to reach the waypoint on time, unless it will be (or already is) late when it runs at maximum velocity. This ensures we never operate near the singularity in line 1. For determining ω_d, we employed a traditional sample-based approach on the input space of angular velocities, and where the linear velocity was fixed at v_d [22]. Thus, given a set of k angular velocity samples where $\omega \in [-\omega_{max}, \omega_{max}]$, a respective set of k trajectories $T(\omega) = [T_1, \ldots, T_k]$ was constructed by integrating the current robot pose forward in accordance with the time-difference equation in (1) over n timesteps associated with the specified control horizon length. Again note that for each trajectory instance $T_i \in T$, the velocity pair (v_d, ω_i) was constant over the control horizon. Defining the set of trajectory endpoints as $T^f(\omega) = [(x_{1n}, y_{1n}), \ldots, (x_{kn}, y_{kn})]$, the desired angular velocity is then specified as

$$\omega_d = \arg\min_{\omega} \|[x_g, y_g]^T - T^f(\omega)\| \quad (3)$$

In other words, the angular velocity associated with the hypothetical trajectory whose endpoint was closest to the target waypoint was chosen. The entire process was then repeated at 10 Hz. While better performance may have been achieved by sampling over the input space of both linear and angular velocities, the optimization problem goes from one dimension to two. As a result, the associated computation would have exceeded the resources available on the PixHawk autopilot. This was the primary motivation of our two-step approach.

V. Experimental Results

Our experimental cycle for LORCA testing had three phases: 1) Software-in-the-Loop (SiL) simulations, 2) Hardware-in-the-Loop (HiL) simulations on an Unmanned Ground Vehicle (UGV), and 3) LORCA field testing. In the first phase, SiL simulations were run first to verify that code behavior is correct. Next, HiL simulations were run using the UGV test mule shown in Figure 5. The motivation for using the UGV was that testing required only a parking lot, and the test-fix-test feedback cycle was much faster than when operating on the water which made development far more efficient. We should also emphasize that HiL testing was a high-fidelity simulation, as both the UGV and LORCA were controlled by the same Pixhawk autopilot. When code was validated on the UGV, the autopilot could be connected to the LORCA without making any changes to the program. Only parameters needed to be changed, (e.g., controller gains, planner horizon time, etc.) and the velocity $\rightarrow$ actuator mappings.

Fig. 5: The UGV used for HiL simulations. This is a Traxxas Slash RC car equipped with a Pixhawk autopilot to enable autonomous operations.

Once performance on the UGV had proven satisfactory, testing moved to the LORCA vehicle and on the water. As alluded to in Section IV, we parameterized a trajectory by a series of 2D waypoints augmented with a desired time of arrival (TOA) at each waypoint. This TOA would correspond to the desired velocity for the vehicle when traveling between waypoints. For safety considerations, our procedure for testing trajectory following was to initiate autonomous operations with the vehicle travelling at a lower speed (e.g., 4 m/s) until it reached the first waypoint to ensure behavior was as expected. Once the first waypoint was achieved, the desired TOA for each subsequent waypoint was updated relative to the actual TOA of waypoint 1, and the vehicle velocity was allowed to increase as necessary. Since the results we present in this paper have target velocities in the 8-10 m/s range, the LORCA was playing catch-up when it started its track. As a result, we ran multiple laps on each trajectory to determine the vehicle's steady-state tracking performance. The results presented below are from laps after the first.

A. Path Following Experiments

Our HiL testing with the UGV was limited to path-following, i.e., there was no specified TOA for the associated waypoints. As a result, the UGV operated at a fixed throttle setting and the planner sampled over the angular velocity space as described in Section IV-C. We found the path following performance of the UGV to be very consistent, with paths across multiple laps effectively overlapping with each other. A representative trial is shown at Figure 6.

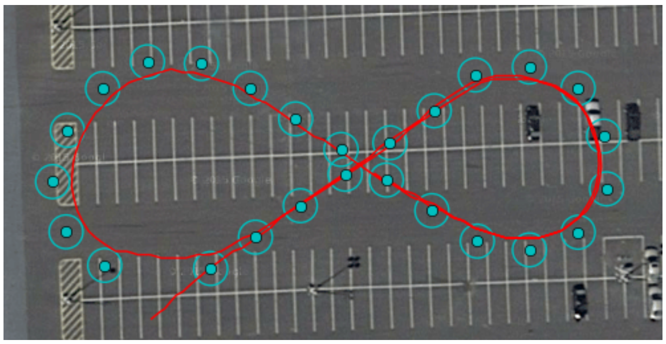

Fig. 6: Figure-eight path following with the UGV. Performance was consistent across multiple laps.

We then attempted to duplicate the performance of the UGV with LORCA on a local pond. However, some modifications to the planner were necessary. These were the result of vehicle dynamics which were unmodeled. Specifically, LORCA is capable of far higher acceleration turns than the UGV. A specified change from low to high angular velocity was effected almost immediately. At times, this would disturb the craft leading to overshoot and oscillations in turns. As a result, we placed constraints on the angular acceleration. These were easily accommodated by the planner by merely constraining the feasible set from which ω was sampled. With these changes, and a subsequent tuning of the control horizon time, LORCA was able to achieve comparable performance on the water to the UGV on the ground. A representative trial is shown at Figure 7. We believe the small amount of algorithmic changes required for migrating from UGV to USV validated our development approach.

B. Trajectory Following

After path following tests were completed, we moved to the Lehigh River in Allentown, PA to evaluate trajectory following performance with TOA requirements at each waypoint. An additional challenge was that the river current (≈ 1 m/s during the days of testing) was unmodeled by our planner.

Our first test featured a 125 meter "oval" which was constructed by connecting two 25 meter radius half-circles with 75 meter straightaways. TOA requirements for each waypoint were determined based upon a constant 8 m/s target velocity for the loop. Results are shown graphically at Figure 8. Overall, performance was quite satisfactory. LORCA was able to follow the path acceptably, and the TOA errors were small ($\mu = 0.1$ s, $\sigma = 0.2$ s).

Fig. 7: Path following in a pond with LORCA. As with the UGV test mule, performance was consistent across multiple loops.

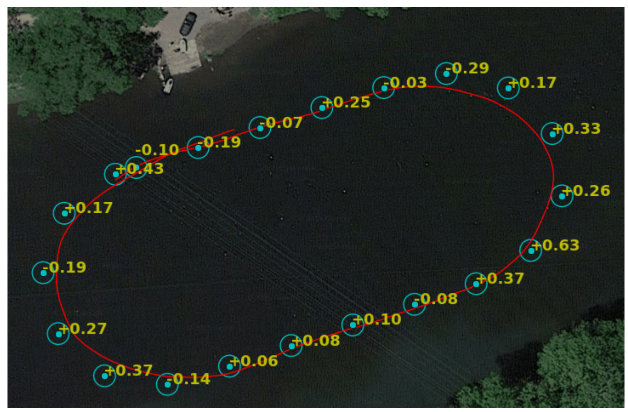

Fig. 8: LORCA trajectory following in the Lehigh river. Beside each waypoint is the TOA error, where a positve difference indicates the LORCA was late to the waypoint. The mean and standard deviation of the TOA error were $\mu = 0.1$ s and $\sigma = 0.2$ s, respectively. Mean and peak speeds for this run were 7.7 m/s and 9.8 m/s, respectively.

To better understand the path taken by LORCA, an explanation of when waypoints are "reached" is warranted. The goal was for the boat to come within a 2.5 m tolerance of each waypoint. However, this was evaluated by the planner based upon the predicted future position of the vehicle using the endpoint of the optimal trajectory in $T^f(\omega)$. The actual vehicle position was not used. Once a waypoint was reached by the planner, the next waypoint was designated as the new target and it would become the goal (x_g, y_g) in (3). As a result, LORCA might not come within the specified tolerance of the actual waypoint even though it was considered reached by the planner. Using Figure 8 as an example, the planner considered all 21 waypoints reached. However, LORCA actually only hit 13 (mean error 1.1 m) and missed 8 (mean error 3.3 m). The average error for all waypoints was 1.9 meters. Note that for calculating the TOA metric, we used the actual time when LORCA reached the waypoint, or in the case of a missed waypoint when it passed closest.

For the next set of experiments, the path was modified to

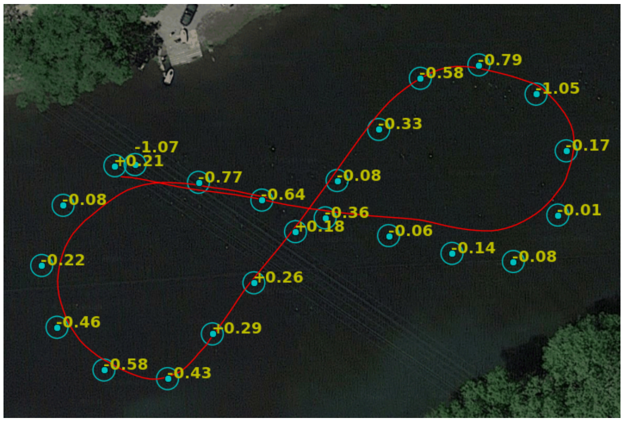

Fig. 9: Trajectory following on a Figure-8. TOA errors were somewhat larger than in the oval case ($\mu = 0.2$ s, $\sigma = 0.4$ s), as was the mean waypoint tracking error (2.8 m vs. 1.9 m). Mean and peak vehicle speeds for this cycle were 9.8 m/s and 13.2 m/s, respectively.

a 125 meter long figure-8 pattern. The motivation was to test something more dynamic by forcing left-to-right and right-to-left turn sequences. Sample results are shown at Figure 9. The target mean velocity for this trial was 10 m/s. In terms of path-following, the performance was slightly worse than the oval track. LORCA hit 13 waypoints (mean error 1.3 m), and missed 10 (mean error 4.6 m). The mean error was 2.8 m for all waypoints (hit and missed). We also noted larger errors and variance with respect to our TOA metric ($\mu = 0.2$ s, $\sigma = 0.4$ s). This was not unexpected, and can be attributed in part to the higher speed and increased dynamics associated with the figure-8 trajectory. We should also point out that the planner had been tuned for operations in the 4-8 m/s range. As a result, despite the shortcomings we feel the trajectory following performance was quite satisfactory with the vehicle reaching peak speeds of 48 km/h on the straighter sections of the figure-8. A video with testing highlights can be viewed at https://www.youtube.com/watch?v=uQc8kZPnKj0.

VI. Discussion

In this paper we introduced LORCA, a high performance USV with applications to surveillance and monitoring tasks. Our initial work in vehicle autonomy produced promising results, especially considering that all computations were on-board the 3DR PixHawk. Despite the simplified vehicle model, our sample-based planning approach yielded satisfactory path following and trajectory tracking performance at relatively high speeds (up to 48 kph). A further advantage of the sample-based approach is that since it is effectively performing numerical integration to predict the future pose of the boat, refinements to the vehicle model can easily be accommodated. We saw this in practice when angular acceleration limits were readily incorporated to smooth the vehicle dynamics.

We acknowledge that our results in autonomy are preliminary. The immediate future will bring additional computational resources to bear so that refinements in planning and control can be made. We will also be integrating exteroceptive sensors suitable for surveillance and monitoring tasks.

Acknowledgments

This work was supported by the Office of Naval Research through a 2013 DURIP grant and Lehigh University 2014 CORE grant. Any opinions, findings, conclusions, or recommendations expressed in this material are those of the author(s) and do not necessarily reflect the views of ONR.

References

[1] P. Rynne and K. von Ellenrieder, "A wind and solar-powered autonomous surface vehicle for sea surface measurements," in *OCEANS 2008*, Sept 2008, pp. 1–6.

[2] H. Ferreira, C. Almeida, A. Martins, J. Almeida, N. Dias, A. Dias, and E. Silva, "Autonomous bathymetry for risk assessment with roaz robotic surface vehicle," in *OCEANS 2009 - EUROPE*, May 2009, pp. 1–6.

[3] J. Manley and S. Willcox, "The wave glider: A persistent platform for ocean science," in *OCEANS 2010 IEEE - Sydney*, May 2010, pp. 1–5.

[4] T. Pastore and V. Djapic, "Improving autonomy and control of autonomous surface vehicles in port protection and mine countermeasure scenarios," *Journal of Field Robotics*, vol. 27, no. 6, pp. 903–914, 2010. [Online]. Available: http://dx.doi.org/10.1002/rob.20353

[5] P. Tokekar, D. Bhadauria, A. Studenski, and V. Isler, "A robotic system for monitoring carp in minnesota lakes," *Journal of Field Robotics*, vol. 27, no. 3, pp. 681–685, 2010.

[6] A. Valada, P. Velagapudi, B. Kannan, C. Tomaszewski, G. A. Kantor, and P. Scerri, "Development of a low cost multi-robot autonomous marine surface platform," in *The 8th International Conference on Field and Service Robotics (FSR 2012)*, July 2012.

[7] S. C. Filippo Arrichiello, Hordur K. Heidarsson and G. S. Sukhatme, "Cooperative caging and transport using autonomous aquatic surface vehicles," *Intelligent Service Robotics*, vol. 5, no. 1, pp. 73–87, Jan 2012. [Online]. Available: http://robotics.usc.edu/publications/759/

[8] M. Dunbabin, "Autonomous greenhouse gas sampling using multiple robotic boats," *Proc. 2015 International Conference on Field and Service Robotics (FSR)*, 2015.

[9] S. Griffith and C. Pradalier, "A spatially and temporally scalable approach for long-term lakeshore monitoring," *Proc. 2015 International Conference on Field and Service Robotics (FSR)*, 2015.

[10] "Liquid robotics - instrument the ocean," http://www.liquidr.com/, accessed: 2015-07-09.

[11] "Maritime robotics," http://www.maritimerobotics.com/, accessed: 2015-07-09.

[12] N. Oceanic and A. Administration, "First underwater robot to cross atlantic highlighted at smithsonian ocean hall," http://www.noaanews.noaa.gov/stories2010/20101208_glider.html, accessed: 2015-07-09.

[13] W. Herkewitz, "Ocean drones plumb new depths," New York Times, Nov 2013.

[14] C. Dobson, J. Mart, N. Strandskov, J. Kohut, O. Schofield, S. Glenn, C. Jones, and C. Barrera, "The challenger glider mission: A global ocean predictive skill experiement," in *IEEE MTS 2013*, 2013.

[15] U. I. O. O. System, "Gliders/autonomous underwater vehicles," http://www.ioos.noaa.gov/glider/welcome.html, accessed: 2015-07-09.

[16] M. Caccia, M. Bibuli, R. Bono, and G. Bruzzone, "Basic navigation, guidance and control of an unmanned surface vehicle," *Autonomous Robots*, vol. 25, no. 4, pp. 349–365, 2008.

[17] P. Encarnaçao and A. Pascoal, "Combined trajectory tracking and path following: an application to the coordinated control of autonomous marine craft," in *Decision and Control, 2001. Proceedings of the 40th IEEE Conference on*, vol. 1. IEEE, 2001, pp. 964–969.

[18] J. P. Hespanha *et al.*, "Trajectory-tracking and path-following of underactuated autonomous vehicles with parametric modeling uncertainty," *Automatic Control, IEEE Transactions on*, vol. 52, no. 8, pp. 1362–1379, 2007.

[19] "3DR Pixhawk Information Portal," http://3drobotics.com/kb/pixhawk/, accessed: 2015-06-29.

[20] T. Perez, T. Fossen, and A. J. Sorensen, "A discussion about seakeeping and manoeuvring models for surface vessels," NTNU, Tech. Rep. MSS-TR-001, 2004.

[21] B. P. Gerkey and K. Konolige, "Planning and control in unstructured terrain," in *ICRA Workshop on Path Planning on Costmaps*, 2008.

[22] S. M. LaValle, *Planning Algorithms*. Cambridge University Press, 2006.